TDEC metric in 50G-PON: analytical and experimental investigation on several implementation aspects

TDEC metric in 50G-PON: analytical and experimental investigation on several implementation aspects

MARIACRISTINA CASASCO[1,5], GIUSEPPE CARUSO[1,2,5], IVAN N. CANO[2], DEREK NESSET[3], MAURIZIO VALVO[4], VALTER FERRERO[1], AND ROBERTO GAUDINO[1]

[1] Politecnico di Torino, Dipartimento di Elettronica e Telecomunicazioni, Torino, Italy
[2] Munich Research Center, Huawei Technologies, Munich, Germany
[3] Ipswich Research Center, Huawei Technologies, Ipswich, United Kingdom
[4] Access Innovation, TIM - Telecom Italia, Torino, Italy
[5] The authors contributed equally to this work
[*] Corresponding authors: mariacristina.casasco@polito.it

Compiled July 1, 2023

We analyze the metrology of TDEC as defined in 50G-PON for assessing transmitter quality. Firstly, we present a theoretical evaluation for adapting TDEC to 50G-PON, where equalized bandwidth limited APD-based receivers are expected. We optimize the parameters for a proper numerical evaluation and provide some guidelines for implementing the metric. We also show that TDEC can be measured with both sampling and real-time oscilloscopes provided that there are enough samples for the latter. A comparison of two techniques, one noiseless and one considering noise enhancement, for computing the coefficients of the equalizer is also provided. Finally, an experimental comparison between a MZM and EML based transmitter is carried out with different extinction ratios and fiber lengths, showing that TDEC can effectively predict the receiver sensitivity penalty.

http://dx.doi.org/10.1364/XX.XX.XXXXXX

1. INTRODUCTION

The continuous demand increase of traffic over broadband connections keeps pushing the available capacity of optical access networks, where the most common technology is passive optical networks (PON). In recent years, the deployment of XG-PON systems with 10 Gbps bitrate has increased [1, 2] and, in order to address a future higher capacity demand, the ITU-T published the recommendation G.9804.3 for 50G-PON physical layer in September 2021 [3].

In order to achieve the high optical loss budgets required (29 dB minimum), a typical implementation for the downstream transmitter (Tx) will most likely use an electroabsorption-modulated laser (EML) followed by an integrated semiconductor optical amplifier (SOA) to boost the optical signal at the optical line terminal (OLT). At the optical network unit (ONU), the receiver (Rx) is expected to be based on 25G-class avalanche photodiodes (APD), since 50G products provide lower gain and are currently not mature enough for commercial deployment. Digital signal processing (DSP) equalization is explicitly considered to overcome the APD bandwidth (BW) limitation and allow compensation of fiber transmission impairments. In addition, DSP can also equalize for Tx imperfections allowing some flexibility of the Tx parameters. It should be considered, however, that having too relaxed Tx parameters can cause operation problems, in case the Rx DSP cannot fully compensate for potential impairments on the transmitted signal. To ensure physical layer interoperability between different Tx and Rx, the transmitter and dispersion eye closure (TDEC) metric was adopted in 50G-PON [3]. TDEC was originally defined in IEEE for non-return to zero (NRZ) signals [4] and extended to four-level pulse amplitude modulation (PAM-4) as TDEC quaternary (TDECQ) [5, 6]. The main advantage of TDEC is that it can assess the performance of a Tx by means of its eye-diagram without explicitly measuring its bit error rate (BER) sensitivity curve with a reference (or "golden") Rx [7].

TDEC in 50G-PON has three main differences with respect to the original metric defined in [4]. Firstly, PONs mainly use APDs to achieve a high power budget. Hence, a variable is added to account for asymmetric noise that is typical for APDs. Secondly, while helping to compensate for the reduced bandwidth of the signal, the Rx equalizer also leads to an increase of the electrical noise. The equalizer noise enhancement factor (C_{eq}), introduced already in TDECQ [8], was also adopted in 50G-PON. The third difference, compared to the IEEE TDEC, is the horizontal location (i.e. the position in time) of the signal histograms which was changed to 0.5 ± 0.075 UI (Unit Interval), to properly take into account the timing jitter that is expected in 50G-PON receivers.

From a system point of view, a high TDEC value indicates

that the Tx eye is not adequately open; then, in order to meet the high power budget requirement in PON, a higher launch optical modulation amplitude (OMA) is needed from the Tx. On the other hand, if the TDEC is very low, then the Tx has a high quality eye-diagram and a lower OMA Tx power can be used. This flexibility allows for the trade-off of parameters such as extinction ratio (ER) and chirp in the Tx and still achieve the PON link budgets. Hence, more optical technologies can comply with the requirements and, as a result, generate a diverse supply chain while still guaranteeing physical layer interoperability [1]. This flexibility allows for the trade-off of parameters such as extinction ratio (ER) and chirp in the Tx while also limiting the permitted variations and still achieve the PON link budgets. Hence more optical Tx technologies can comply with the requirements and, as a result, generate a diverse supply chain provided that they have enough quality, i.e. within the acceptable TDEC values. Physical layer interoperability is then guaranteed for Rx that are at least as powerful as the minimum Rx specified in TDEC. In the G.9804.3 standard, a maximum value (up to 5 dB) is set for TDEC to guarantee a minimum quality level of the Tx, when considering a given reference band-limited and equalized receiver (as also explained in [9]). Beyond this value, the TDEC metric starts diverging from the OMA penalty, hence becoming less reliable [10].

In this paper, we study the metrology aspect for TDEC and carry out an evaluation and optimization of several variables. The main objective is to provide some guidelines when implementing TDEC. The paper is organized as follows: firstly, we introduce TDEC and validate theoretically the asymmetric noise factor introduced for APD Rx. We then optimize several parameters, e.g. number of samples per bit, number of histograms and step size, for TDEC numerical evaluation and provide the minimum values needed for a converged TDEC value. Afterwards, we demonstrate that with digital upsampling and real-time oscilloscopes (RTO), we can obtain TDEC values comparable with the ones from digital sampling oscilloscopes (DSO). We also investigate two types of optimization for the linear equalizer coefficients (usually named in literature as "zero forcing" (ZF) or "minimum mean square error" (MMSE)). Finally, an experimental comparison between between Mach-Zehnder Modulator (MZM) and EML-based Tx is also done for different extinction ratio and fiber lengths, showing that TDEC, without requiring explicit BER evaluation, effectively predicts Rx sensitivity penalty in all cases of interest in 50G-PON.

2. INTRODUCTION TO THE TDEC PARAMETER

The idea behind the TDEC metric is to estimate the maximum amount of noise that can be added to a detected optical signal until a target BER is reached and then compare it with an ideal case. Starting from a theoretical BER computation, the noise value, namely σ_G, is computed in an iterative way by evaluating eq. (9-3) of [3] as:

$$\frac{1}{2}\left(\frac{\int f_u(y)\,\mathrm{Q}\left(\frac{y-P_{avg}}{C_{eq}\cdot\sigma_G(y)}\right)dy}{\int f_u(y)dy}\right) + \frac{1}{2}\left(\frac{\int f_l(y)\,\mathrm{Q}\left(\frac{P_{avg}-y}{C_{eq}\cdot\sigma_G(y)}\right)dy}{\int f_l(y)dy}\right) = BER_{target} \quad \textbf{(1)}$$

Here $f_u(y)$ and $f_l(y)$ are the upper and lower distributions of the samples captured in an oscilloscope, representing each of the two levels of the NRZ signal. $Q(x)$ measures the area under a normal curve for values greater than x. BER_{target} is the pre-forward error correction (FEC) BER threshold, i.e. 10^{-2}. P_{avg} is the average power of the signal, $\sigma_G(y)$ is the noise standard deviation added to the detected signal; this term depends on the power level of the sample and it is defined in eq. (9-4) of [3] as:

$$\sigma_G(y) = \sqrt{\left(M^2(y)\left(\sigma_{0,G}^2 + S^2\right) - S^2\right)} \quad \textbf{(2)}$$

where $M(y)$ is the power-dependent noise asymmetry factor, $\sigma_{0,G}$ is the noise that is added to the signal and S is the standard deviation of the oscilloscope noise when no signal is applied.

The recommendation for 50G-PON assumes an equalizer to compensate for fibre link and limited BW Rx. TDEC emulates the latter with a low-pass filter and then considers the noise-enhancement effect of the equalizer through the C_{eq} parameter, defined in eq. (9-6) of [3] as:

$$C_{eq} = \sqrt{\frac{N_0}{2}|H_{Bessel}|^2 \cdot |H_{eq}|^2} \quad \textbf{(3)}$$

where $N_0/2$ is the noise spectrum, H_{Bessel} is the transfer function of a fourth-order Bessel-Thomson filter with a 3-dB BW of 18.75 GHz, representing the 25G-class APD, and H_{eq} is the transfer function of the equalizer. The latter is derived from the 13 T-spaced taps optimised to give the minimum mean square error according to equation (9-7) in [3].

In order to account for any eye distortion, the procedure evaluates two separate noise values, one to the left (σ_L) and one to the right (σ_R) side of the eye center, respectively at 0.425 UI and 0.575 UI. This means that overall, there are four different locations in the eye diagram where the noise must be added: left and right of the centre of the eye, each for the upper and lower distribution, as depicted in Fig. 1(a). The reference time window is computed by averaging the time instants where the sample power reaches the average power [4]. For the device under test, the amount of noise to be kept in account is $\sigma_G = min(\sigma_L, \sigma_R)$. Subsequently, the noise that can be added to an ideal signal (i.e. noiseless and without distortions) is calculated. This value is referred to as σ_{ideal} and can be found numerically from eq. (9-9) of [3] as:

$$2 \cdot BER_{Target} = Q\left(\frac{OMA}{2\sigma_{ideal}}\right) + Q\left(\frac{OMA}{2m\sigma_{ideal}}\right). \quad \textbf{(4)}$$

Here $OMA = P_1 - P_0$ (where P_1 and P_0 are computed following [3]), m is the asymmetry noise factor and Q is defined as [11]:

$$Q(x) = \frac{1}{2}\,\mathrm{erfc}\left(\frac{x}{2}\right). \quad \textbf{(5)}$$

In the end, the TDEC metric is obtained as a ratio between σ_G and σ_{ideal}, that is:

$$TDEC = 10 \cdot log\left(\frac{\sigma_{ideal}}{\sigma_G}\right). \quad \textbf{(6)}$$

Fig. 1(b) summarizes the procedure just described. We call *Method A* the computation of TDEC using eq. 6, where σ_G derives from eq. 1 with C_{eq}.
In case C_{eq} cannot be directly obtained from the instrument, the recommendation [3] defines an alternative method for evaluating TDEC. Here, the target BER is evaluated following eq. 1

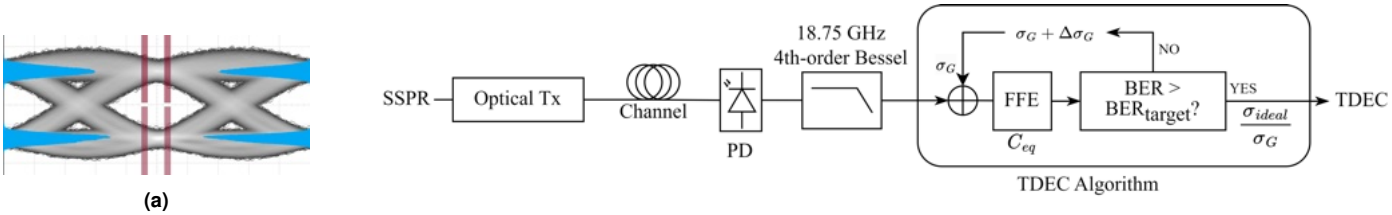

(a) (b)

Fig. 1. (a) Eye diagram showing the four sampling windows and the resulting histograms. (b) Block diagram summarizing the TDEC evaluation procedure.

neglecting the C_{eq} term, and then by adding it in a second step as in eq. (9-11) of [3]:

$$TDEC = 10 \cdot log_{10}\left(C_{eq}\frac{\sigma_{ideal}}{\sigma_G}\right). \quad (7)$$

We call *Method B* the TDEC calculation using eq. 7, with σ_G obtained by setting $C_{eq} = 1$ in eq. 1 (as if no equalizer is present).

3. TDEC EXTENSION FOR APD RECEIVERS

In 50G-PON, the Rx will very likely employ APDs to obtain sufficiently good sensitivity for achieving the high power budgets needed [3]. In APDs, the avalanche gain mechanism has the consequence of producing a higher noise level on the "1" level (with power P_1) with respect to the "0" level (with power P_0) [12]. In order to take into account this imbalance, the noise asymmetry variable m is defined as [3]:

$$m = \frac{\sigma_1}{\sigma_0} \quad (8)$$

where σ_0 and σ_1 are the noise standard deviations for the low and high level, respectively. In order to define a value for m, we can consider that each noise term consists of a shot noise (σ_{sh}) and a thermal noise (σ_{th}) component, independent from each other [12], such that

$$\sigma_{0,1} = \sqrt{\sigma^2_{sh_{0,1}} + \sigma^2_{th}} \quad (9)$$

In particular, σ_{sh} depends directly on the power level, according to the following model:

$$\sigma^2_{sh_{0,1}} = 2qG_A^2F_GR\Delta f \cdot P_{0,1} \quad (10)$$

where q is the electron charge, G_A is the avalanche gain of the photodiode (PD), F_G is the excess noise factor, R is the PD responsivity and Δf is the receiver electrical bandwidth. All the terms in 10 may be considered constant, with the exception of the power level.

The ER of the received signal can be expressed as

$$ER = \frac{P_1}{P_0} \quad (11)$$

If we define the ratio of the thermal to the shot noise in the "1" level as:

$$\rho_1 = \frac{\sigma^2_{th}}{\sigma^2_{sh1}} \quad (12)$$

we can substitute 9, 10, 11 and 12 into 8, obtaining:

$$m = \sqrt{\frac{1+\rho_1}{\frac{1}{ER}+\rho_1}} \quad (13)$$

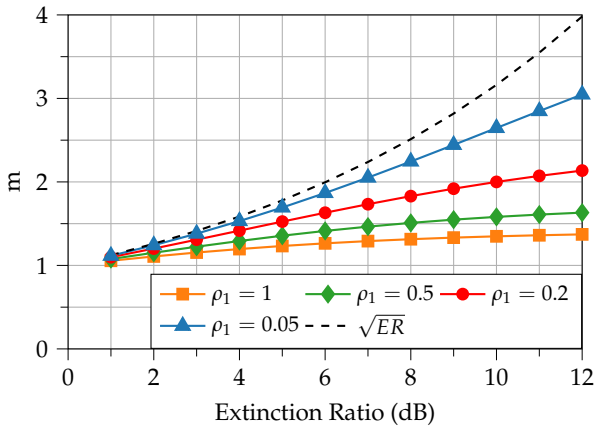

Fig. 2. Asymmetric noise value (m) against ER for several values of ρ_1

eq. 13 shows the relation between the ER and the asymmetry noise factor m. For a p-i-n PD, thermal noise σ^2_{th} is the dominant term, which results in $\rho_1 \gg 1$ and leads to $m = 1$ (lower bound). In an avalanche shot noise limited Rx (which is the case for APDs working in low error rate conditions, e.g. BER $\approx 10^{-10}$), instead, we get $\rho_1 \ll 1$, which leads to the noise asymmetry value becoming dependent on the ER as $m = \sqrt{ER}$. This relation is represented by the dashed line of Fig. 2 and can be considered as the upper bound.

At a pre-FEC BER level of 10^{-2}, however, the signal power is so low that σ^2_{th} becomes non negligible and even comparable to the shot noise. Fig. 2 plots the value of m against ER for different values of ρ_1. We can observe that in the range $0.2 < \rho_1 < 1$ the value of m is bound between 1 and 2.5, depending on the ER. Moreover, when going to the limit of ER $\to \infty$, m tends to converge. Hence, for values of ER up to 8 dB, the asymmetric noise is in the range $1 < m < 2$. In the current 50G-PON recommendation, a value of 1.5 has been selected.

In order to account for the different sample power values that appear inside a histogram, the value of m is adapted accordingly. A linear relation between m and power can be adopted, considering $m = 1$ for the 0-level and $m = 1.5$ for the 1-level. Then, the following equation is obtained from eq. (9-5) of [3]:

$$M(y) = \begin{cases} \frac{m(y-y_0)+(y_1-y)}{y_1-y_0} & \text{for } y \geq y_0 \\ 1 & \text{for } y < y_0 \end{cases} \quad (14)$$

The value of M depends on the power of the sample and is used in eq. 2.

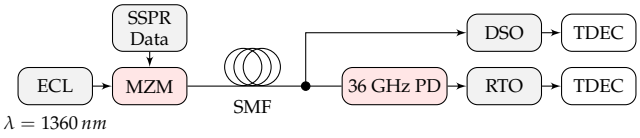

Fig. 3. Experimental setup for TDEC measurements

4. OPTIMIZATION OF SOME PARAMETERS IN THE TDEC ALGORITHM IMPLEMENTATION

In this section, we discuss the optimization of several parameters appearing in G.9804.3 TDEC definition.

A. Experimental setup

For our tests, we implement the experimental setup depicted in Fig. 3. All the experiments are carried out at a bitrate of 50 Gbps. An O-Band Mach-Zehnder modulator (MZM) converts a short stress pattern random (SSPR) stream [13] into an optical NRZ signal. The light source is an external cavity laser (ECL) emitting at 1360 nm. Such wavelength is used to emulate the highest accumulated CD (77.1 ps/nm) after 20 km of G.652 fiber at the longest 50G-PON downstream wavelength, i.e 1344 nm. The optical signal ER is limited to 9 dB and it is sent through a standard single mode fiber (SMF).

At the Rx, the signal is either captured directly using the optical input of a digital sampling oscilloscope (DSO) or we use a 36 GHz PIN PD to perform optical to electrical conversion and obtain the samples through a real-time oscilloscope (RTO). For both oscilloscopes, an external clock recovery module is used.

We evaluate TDEC with both the RTO and DSO. With the latter (Keysight N1092C), we directly measure the TDEC from the algorithm embedded in the instrument. Instead, with the RTO (Tektronix DPO70000SX) we acquire the waveform and compute the TDEC offline with an algorithm implemented in MATLAB.

B. TDEC Practical Parameters optimization

In order to assess the optimization for TDEC, we implement the algorithm offline and vary some parameters. We use an SSPR signal (32762 bits) acquired from the RTO (with 4 Sa/bit) and upsample it to 32 Sa/bit for having enough granularity. The TDEC algorithm has several parameters that need to be properly evaluated in order to obtain a consistent value. The procedure depends on the following: average power (P_{avg}) computation, the number of bins (N_{bins}) for each of the four histograms and noise power increment. The procedure for assessing P_{avg} is defined in [3]. Low and high power levels are measured over sequences of 72 consecutive 0 or 1, present in the SSPR test signal, and afterwards P_{avg} is obtained as the average of the two values. After computing P_{avg}, we then optimize N_{bins}. For this purpose, we first find the minimum and maximum signal level for each of the four sampling locations and then create a histogram with N_{bins}.

Fig. 4 plots the resulting TDEC vs. N_{bins}. If $N_{bins} < 30$, the TDEC is overestimated, since we introduce a sort of quantization error (the power levels are rounded to the central value of the histogram bin). On the other hand, for $N_{bins} > 30$ TDEC changes marginally, however with an increased computation time. For the rest of the evaluations we employ $N_{bins} = 50$. The noise power step increment $\Delta\sigma_G$ is important in the iterative evaluation of eq. 1. Fig. 5 shows TDEC against $\Delta\sigma_G$, which we express as a fraction of P_{avg}. As expected, TDEC is underestimated when an exceedingly large $\Delta\sigma_G$ is used, since the noise value will quickly produce the BER_{target}. From Fig. 5, we see that $\Delta\sigma_G < P_{avg}/500$ is needed to provide a converged TDEC value. As a good trade-off between speed and accuracy, we use $\Delta\sigma_G = P_{avg}/5000$ for the rest of the offline measurements.

Finally, we test both *Method A* and *Method B* described in Section 2 and obtain a marginal difference of 0.03 dB in the TDEC values. Hence, the two methods are equivalent.

5. TDEC EVALUATION USING REAL-TIME AND SAMPLING OSCILLOSCOPES

Two families of oscilloscopes can be used to acquire ultra high frequency waveforms: DSOs, also known as equivalent-time oscilloscopes, and RTOs [14]. The first one samples periodic waveforms every $T_p + \Delta_{DSO}$, where T_p is the waveform period and Δ_{DSO} is a small time displacement to capture the signal at a slightly different point in each period. On the other hand, RTOs do not require periodic waveforms and sample uniformly over time using high speed analog to digital converter (ADC) and ultra-fast memory storage, capturing one sample every Δ_{RTO} seconds. For instance, when sampling a 50 Gbps signal, a 200 GSamples/s RTO continuously acquires 4 samples/bit uniformly spaced Δ_{RTO}=5 ps, storing them in an internal random access memory (RAM) for the following post-processing and display. An illustration of the two operating principles is shown in Fig. 6.

Currently, the state-of-the-art DSO can achieve very precise and small Δ_{DSO} and typically $\Delta_{DSO} \ll \Delta_{RTO}$, so that DSOs present a higher temporal resolution compared to RTOs, at the expense of requiring a periodic signal [15]. We compare the TDEC on waveforms captured with the two oscilloscope types, as in Fig. 3. For the RTO, we convert the optical signal to the electrical domain by means of a 36 GHz PIN PD and capture it at a sampling rate of 200 GSa/s. It is clear that with this limited amount of samples the two histogram time windows cannot be properly determined. We thus digitally upsample the waveform to N_{up} samples/bit using anti-aliasing filter approximated with Kaiser window method. In this way we go from the initial 4 samples/bit to N_{up} samples/bit. Fig. 7 shows the TDEC value vs. N_{up}. We also plot value obtained with a DSO having Δ_{DSO}=200 fs (green line). It can be noticed that the TDEC estimates obtained by upsampling the RTO output converge almost perfectly to the DSO value provided that at least

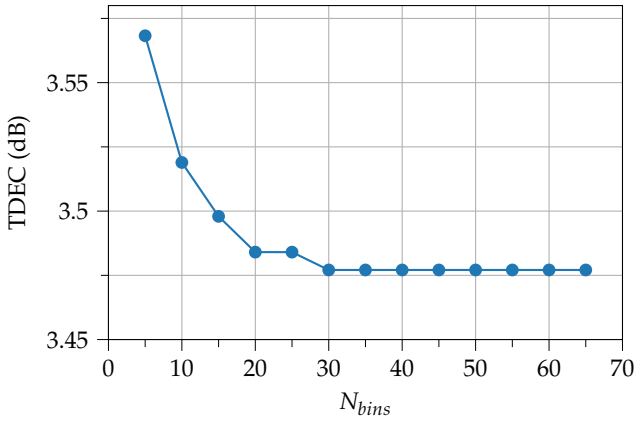

Fig. 4. TDEC vs. number of histogram bins (N_{bins})

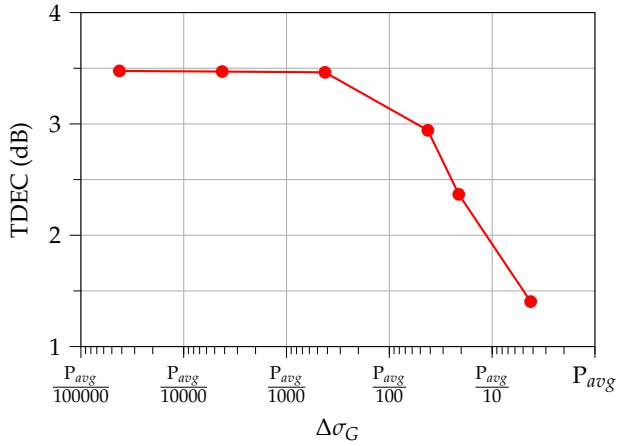

Fig. 5. TDEC dependency on the noise step size $\Delta\sigma_G$.

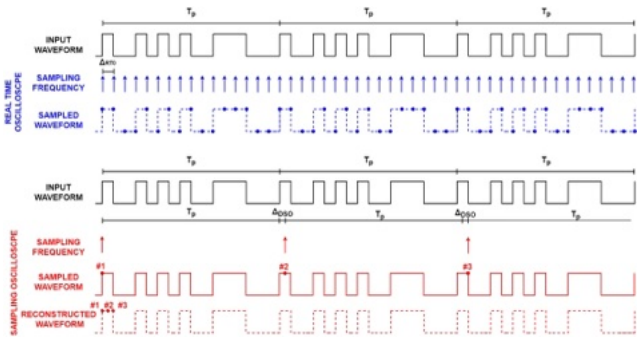

Fig. 6. Difference between the two sampling modes of real-time oscilloscopes (blue) and the sampling (red) of the same input waveform (black).

N_{up}=16 samples/bit are used. This is reasonable, since with N_{up}=16 we have Δ_{RTO}=1.25 ps, which corresponds to 0.0625 UI and is close enough to the 0.04 UI histogram width specified in the ITU-T standard [3]. Moreover, with this choice, the left and right histogram end up being located at 0.4375 and 0.5625 UI, respectively, again very close to the sampling windows from the standard (0.425 and 0.575 UI). Choosing a higher value for N_{up} changes the resulting TDEC estimate only marginally, so we can conclude from Fig. 7 that N_{up}=16 samples/bit is a reasonable value.

As final observation, for sufficiently high N_{up}, the RTO TDEC estimate is around 0.1 dB lower than the DSO. We can justify this mismatch in several ways ways: first, the difference in the specifications of the two oscilloscopes, in terms of analog bandwidth and effective number of bits; then, for the RTO case we use a commercial PD, which has a non-ideal frequency response, whereas for the DSO the Rx module is well calibrated; last, the digital upsampling is an ideal operation, which does not take into account the noise.

6. ZERO FORCING (ZF) AND MINIMUM MEAN SQUARE ERROR (MMSE) EQUALIZER STRATEGIES

The recommendation of the 50G-PON [3] employs a 13-taps T-spaced FFE whose taps coefficients are optimized to give the MMSE for eye opening. In the literature, we typically find two algorithms to compute the FFE coefficients [16, 17]:

1. Zero-Forcing (ZF), where the taps are optimized to obtain zero inter-symbol interference (ISI) on the equalized eye diagram without considering the presence of noise on the input signal.

2. Minimum Mean Square Error (MMSE), that maximizes the signal-to-noise ratio at the equalizer outputs jointly considering ISI and noise on the input signal.

When using ZF, the FFE taps optimization algorithm minimizes the ISI at the equalizer output. Fig. 8(a) illustrates the principle of this equalizer. In order to optimize the coefficients in time domain, we use an adaptive stochastic gradient descent [17] with a step size of 10^{-3} after normalizing the input samples to be in the range [-1,+1]. We train the equalizer with 2^{14} bits. To find the best sampling instant, we repeat the taps optimization N times (with N being the number of samples per bit) and then we select the one giving the minimum TDEC value. In Fig. 9 we show the TDEC values against each sampling instant when $N = 32$ is used. We observe a typical bath-tub curve and, as expected, the optimal sampling instant is close to the middle. Similar observations are reported in [18]. After finding the taps corresponding to best sample instant, we use them to filter 3 consecutive SSPR sequences for TDEC evaluation.

For the MMSE strategy, we add time-domain Gaussian noise samples and optimize the taps according to the MMSE criterion. We evaluate the BER and iterate the process increasing the input noise variance until the target BER of 10^{-2} is reached. Also in this case, we repeat the process for each sampling instant and select the sample where the highest noise variance can be added, using the same sequences and step size as before. We then evaluate TDEC for this sample and from it, we implement a FIR filter with these taps for the equalization. The block diagram is shown in Fig. 8(b).

We experimentally test both ZF and MMSE equalizer with an SSPR sequence [13]. Here, we use an RTO and the captured 4 samples/bit waveform is then oversampled to 32 via digital interpolation. The samples are then filtered with a 4th order low-pass Bessel filter with 3-dB BW of 18.75 GHz ([3]) and equalized following ZF and MMSE approaches. The resulting TDEC and C_{eq} values are reported in Table 1 for the two cases.

Both equalizers give quite similar TDEC values, with MMSE giving a value 0.17 dB lower than ZF. However, a significant

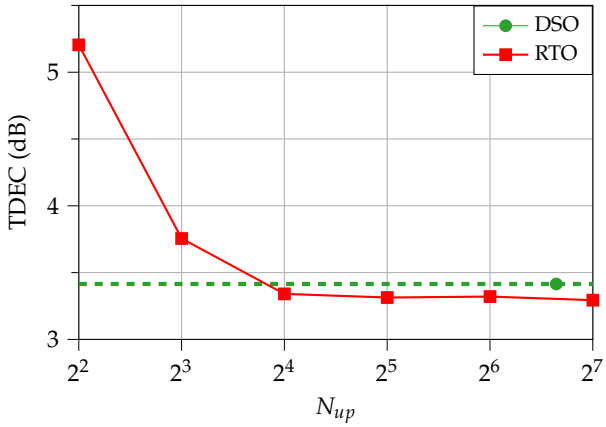

Fig. 7. TDEC vs. N_{up} (samples per symbol after upsampling in for the RTO). The DSO reference TDEC value (for $\Delta_{DSO} = 200fs$) is reported as a green line as a comparison.

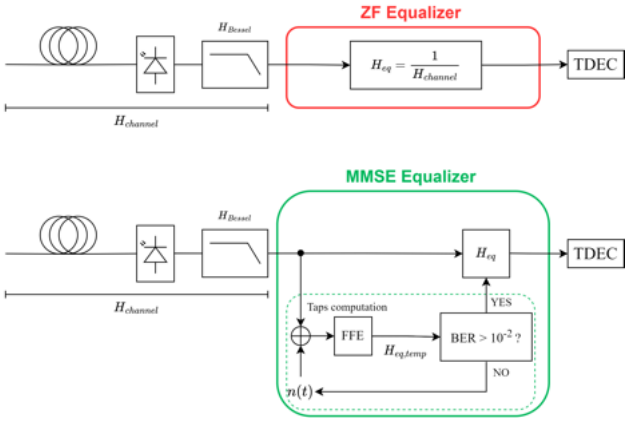

Fig. 8. Block diagram of the two equalization techniques: (a) Zero Forcing (ZF) equalizer and (b) Minimum Mean Square Error (MMSE) equalizer.

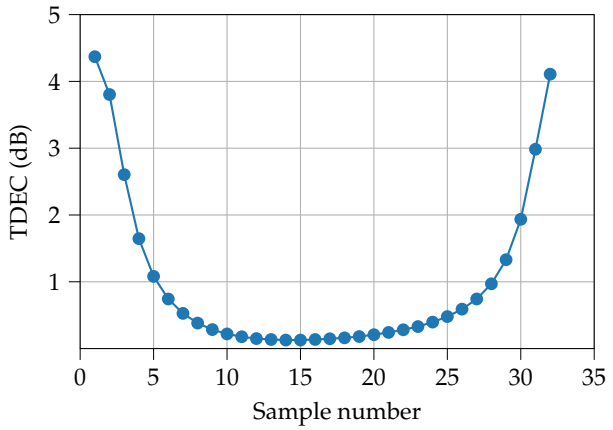

Fig. 9. TDEC vs. sampling instant position for the ZF tap optimization strategy

variation is visible in the C_{eq}, as expected from theory. The ZF equalizer tries to minimize ISI at the FFE output, regardless of noise. For a typical BW-limited channel, it tends to enhance the high frequency components not only of the signal, but also of the noise, which is reflected in a higher C_{eq}. On the other hand, the MMSE jointly minimizes ISI and noise, limiting the noise enhancement and consequently obtaining a lower C_{eq}. In Fig. 10 we show the non-equalized experimental eye-diagram and the equalized eye-diagrams using the two methods. A larger eye opening can be seen after the ZF equalizer compared to MMSE, at the expense of increased noise at high frequencies; this is noticeable from a higher standard deviation at the bit transitions (Fig 10(b)).

In order to further evaluate the ZF and MMSE strategies, we carry out a series of simulations. We emulate the bandwidth

Table 1. ZF and MMSE results

	$TDEC$ (dB)	C_{eq} (dB)
ZF	3.47	3.29
MMSE	3.30	2.49

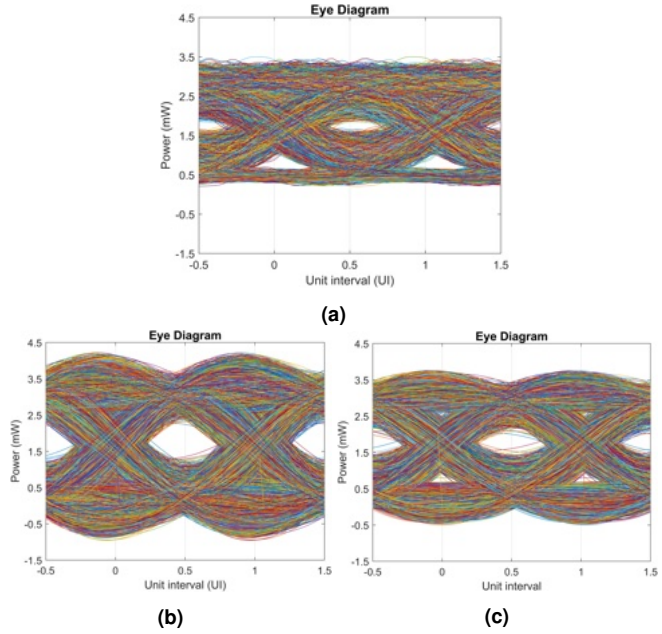

Fig. 10. Eye-diagrams from experimental data. (a) Back-to back received waveform (b) Waveform after ZF equalizer (c) Waveform after MMSE equalizer

of an optical transmitter using a 2nd-order Butterworth filter where we change the 3-dB BW. We use an SSPR sequence [13] oversampled to 4 samples/bit to emulate the RTO and compute TDEC and C_{eq} as previously described.

Fig. 11 depicts TDEC and C_{eq} for the two equalization strategies (ZF in red, MMSE in green) when changing the Tx 3-dB BW. The plots indicate that when there is enough BW ($\approx$ 30 GHz), both ZF and MMSE produce the same TDEC and C_{eq}. As the BW reduces, the MMSE equalizer produces a slightly lower TDEC, as it also takes noise into account. This is more evident when looking at the C_{eq} curve in Fig 11(b), where the ZF strategy significantly enhances the noise. The different effect of the two equalizers can be clearly seen when looking at the insets of Fig 11(b) linked to the lowest BW. The results show that both ZF and MMSE can be used correctly for TDEC evaluation, as they provide similar TDEC values. Although ZF strategy is faster and easier to implement than the MMSE strategy, it is left to the metrology expert to choose and optimise based on his handwork.

Both ZF and MMSE provide a similar TDEC value, despite the C_{eq} difference at low BW. While ZF is faster and simpler to implement than MMSE, it is left to the metrology experts to choose the tap optimization strategy according to their hardware.

7. EXPERIMENTAL VERIFICATION OF THE CORRELATION BETWEEN TDEC AND OMA SENSITIVIY PENALTY

In this last section, we experimentally verify in a realistic setup if the TDEC effectively predicts OMA sensitivity penalty (OMA_{pen}) at the target BER when changing ER, fiber length and thus accumulated chromatic dispersion (CD) and also for different kinds of transmitters. The correlation between TDEC and OMA_{pen} is the main motivation for introducing this metric.

The setup is depicted in Fig. 12. We employ the same MZM

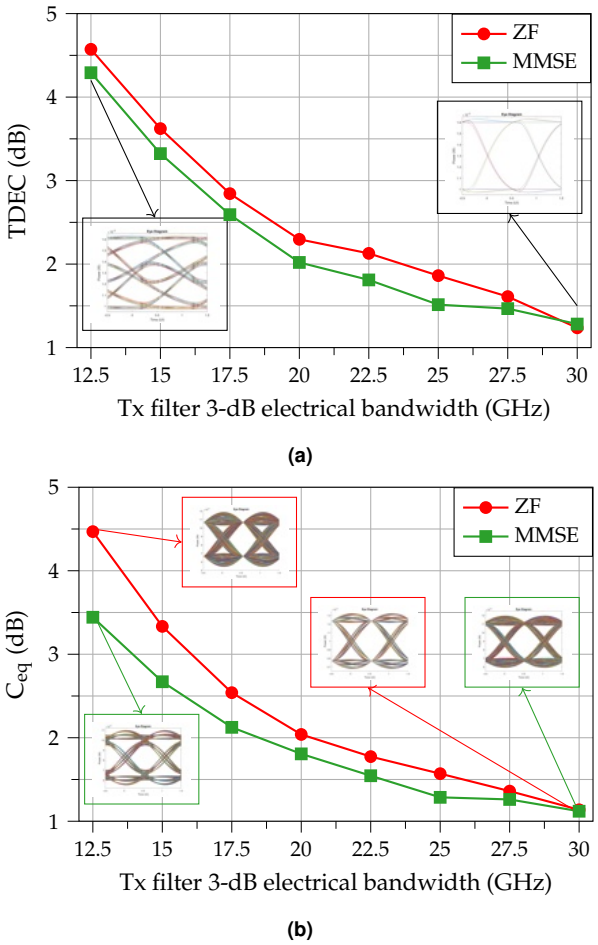

Fig. 11. TDEC (a) and C_{eq} (b) against 3-dB electrical BW for ZF and MMSE equalizer. Insets of (a) report the eye-diagrams before equalization at the highest and lowest BW under test. Insets of (b) show the eye diagrams after ZF and MMSE equalization

as in Fig. 3 and for comparison we also test a 25G-class EML emitting at 1299 nm. We add different lengths of SMF to evaluate several CD values. We directly capture the optical signal by means of a DSO and then process it to compute the TDEC. For this set of experiments, we only report the results obtained directly from the DSO. For the Rx sensitivity, we employ a 25G-class APD preceded by a variable optical attenuator (VOA) to control the input power. The electrical signal is then sampled at 8 Sa/bit by the DSO and equalized with a 13-tap T-spaced FFE as required by the 50G-PON standard. Afterwards, we perform the symbol decision and compute the BER at the best sampling instant.

In a first round of experiments we focus on the dependence on the ER parameter. To this end, we measure the TDEC and the Rx OMA sensitivity at pre-FEC target BER=10^{-2} in back-to-back (BtB), varying the transmitted signal ER from 5 dB to 9 dB in steps of 1 dB. These ER values are reasonable for an EML-based Tx at the OLT. We also change the asymmetric noise parameter m in the TDEC formula to validate the range considered in Section 3. The results are plotted in Fig. 13, where a clear relation between the two measurements is visible. We thus evaluate the linear regression on the points for m = 1, 1.5, 2 and 3 and the resulting slopes are 1.1, 0.97, 0.52 and 0.28 (with a statistical R^2

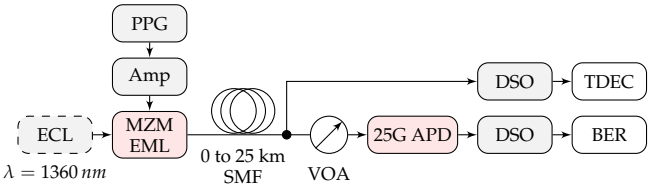

Fig. 12. Setup for TDEC and Rx sensitivity measurements

parameter respectively equal to 0.93, 0.92, 0.90 and 0.86). This graph confirms the choice of m = 1.5 in the ITU-T standard for 50G-PON, since it gives slope and R^2 very close to 1.

In another set of experimental tests, we fix ER=7 dB and $m = 1.5$ and measure the relation between TDEC and Rx sensitivity when varying the accumulated CD of the link. We change the fiber length from BtB to 25 km in 5 km steps and show the results in Fig. 14. The path penalty obtained with TDEC and Rx sensitivity after 25 km with respect to BtB is almost identical (≈1.4 dB). Furthermore, when correlating the two metrics, a linear regression yields a slope of 0.97 and an R^2 of 0.923, indicating a very good correlation between the two variables.

For comparison, we also tested an EML as the Tx, since these devices are more common in the PON application. Fig. 14 includes the EML results of TDEC against OMA at BER=10^{-2} from BtB to 25 km. Since TDEC is a metric that indicates the Tx quality, we expect it to indicate a difference between using EML and MZM. In BtB, the measured TEC is 2.2 dB and 2.4 dB for MZM and EML respectively, with corresponding OMA Rx sensitivity of -24.1 dBm and -23.9 dBm. Remarkably, TDEC perfectly follows the Rx sensitivity penalty, demonstrating that it is a useful metric for Tx qualification. From Fig. 14 we observe that TDEC and OMA Rx sensitivity with the EML improve after SMF. This behavior is explained by the combined effect of the EML positive chirp and of the emission wavelength (1299 nm) being in the negative CD regime, which causes a pulse compression [19] and opens the eye-diagram after fiber transmission. This effect is more evident in [20], where a directly modulated laser (DML) at 1293 nm is employed as Tx. Furthermore, after 20 km the measured TDEC and OMA Rx sensitivity are 1.8 dB and -24.45 dBm respectively, which are 0.5 dB and 0.45 dB better than in BtB, indicating that TDEC and Rx sensitivity variation go together hand-in-hand. In addition, when doing a linear regression, the

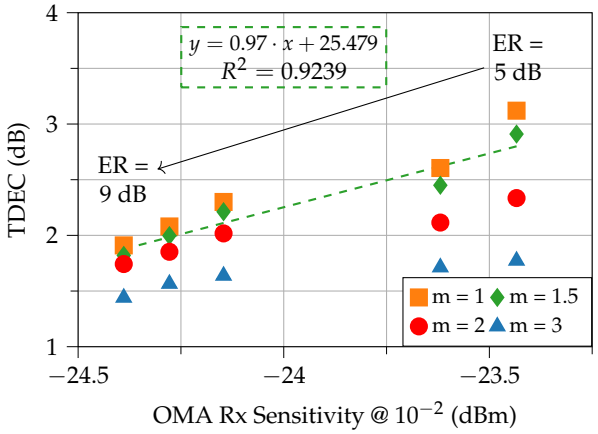

Fig. 13. TDEC vs. OMA Rx sensitivity for different values of m and Tx ER. Dashed line shows the linear trendline for $m = 1.5$

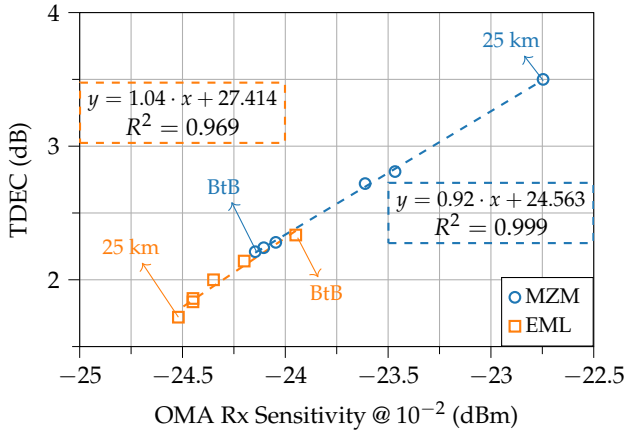

Fig. 14. TDEC against OMA Rx sensitivity for several fiber lengths (steps of 5 km). Inset boxes show regression line and R^2 coefficient for MZM (blue) and EML (orange)

slope is 1.04 indicating again a good correlation between the variables. Hence, TDEC clearly follows the Rx sensitivity and is a good indicator of the penalty that the system can experience after fiber transmission.

8. CONCLUSIONS

In this paper we studied the metrology for TDEC defined for 50G-PON. We provided a theoretical derivation of the excess noise factor in APDs, commonly used in PON Rx, validating the value of 1.5 inside the TDEC equation. We optimized N_{bins} of the histograms at each of the sampling points defined within the eye-diagram and determined that $N_{bins} = 40$ is enough for a reliable TDEC value. We also found that $\Delta\sigma_G \leq P_{avg}/5000$ is adequate for a precise TDEC.

A comparison between RTO and DSO indicated that the captured waveform from an RTO requires a digital oversampling to at least 32 samples/bit to obtain the same TDEC value as with a DSO. We tested a zero forcing and a minimum mean square error approach to compute the equalizer taps. Both methods resulted in a similar TDEC value, however the C_{eq} in the zero forcing equalizer was higher, since it enhances not just the higher frequency signal components, but also the noise.

Finally, we evaluated the relation between TDEC and OMA Rx sensitivity using a MZM at Tx. We varied the ER and the fiber length, and the results showed a correlation close to 1 between TDEC and OMA Rx sensitivity. We also assessed an EML emitting in the negative CD regime; the transmission after different fiber lengths gave again a correlation close to 1. These results show that the variation in TDEC can be directly translated into OMA penalty and, thus, TDEC can evaluate the Tx quality and help to guarantee transceiver interoperability.

REFERENCES

1. R. Bonk, D. Geng, D. Khotimsky, D. Liu, X. Liu, Y. Luo, D. Nesset, V. Oksman, R. Strobel, W. Van Hoof, and J. S. Wey, "50G-PON: The First ITU-T Higher-Speed PON System," IEEE Commun. Mag. **60**, 48–54 (2022).
2. D. Nesset, "The Progress of Higher Speed Passive Optical Network Standardisation in ITU-T (invited)," in 2021 European Conference on Optical Communication (ECOC), (2021), pp. 1–4.
3. ITU-T, "G.9804.3 : 50-Gigabit-capable passive optical networks (50G-PON): Physical media dependent (PMD) layer specification," https://www.itu.int/rec/T-REC-G.9804.3-202109-I.
4. IEEE, IEEE Standard for Ethernet (IEEE, 2018), Sec. 6, Clause 95: Physical Medium Dependent (PMD) sublayer and medium, type 100GBASE-SR4, pp. 558–561.
5. J. King, D. Leyba, and G. D. LeCheminant, "TDECQ (Transmitter Dispersion Eye Closure Quaternary) replaces historic eye-mask and TDP test for 400 Gb/s PAM4 optical transmitters," in 2017 Optical Fiber Communications Conference and Exhibition (OFC), (2017), pp. 1–3.
6. S. Echeverri-Chacón, J. J. Mohr, J. J. V. Olmos, P. Dawe, B. V. Pedersen, T. Franck, and S. B. Christensen, "Transmitter and Dispersion Eye Closure Quaternary (TDECQ) and its sensitivity to impairments in PAM4 waveforms," J. Light. Technol. **37**, 852–860 (2019).
7. J. Petrilla, P. Dawe, and G. D. LeCheminant, "New metric offers more accurate estimate of optical transmitter's impact on multimode fiber-optic links," in DesignCon 2015, (2015).
8. IEEE, IEEE Standard for Ethernet (IEEE, 2018), Sec. 8, Clause 121: Physical Medium Dependent (PMD) sublayer and medium, type 200GBASE-DR4, pp. 131–136.
9. D. van Veen, R. Borkowski, A. Mahadevan, and V. Houtsma, "Interoperability and Experimental Evaluation of TDEC(Q) Testing for 50 and 100G PONs," in 2023 Optical Fiber Communications Conference and Exhibition (OFC), (2023), pp. 1–3.
10. Y. Zhao, C. Doerr, L. Chen, N. Zhu, D. Ton, R. Aroca, X. Huang, and M. Xu, "BER and TDECQ Correlation for Different Impairments in 400Gbps PAM4 System," in 2020 Optical Fiber Communications Conference and Exhibition (OFC), (2020), pp. 1–3.
11. J. R. Proakis and M. Salehi, Digital Communications (McGraw-Hill Higher Education, 2008), chap. 2: Deterministic and Random Signal Analysis, pp. 17–94, 5th ed.
12. G. P. Agrawal, Fiber-Optic Communication Systems (Wiley, New York, 2010), chap. 4: Optical Receivers, pp. 128–181, Wiley series in Microwave and Optical Engineering, 4th ed.
13. OIF-CEI, "Implementation agreement OIF-CEI-04.0 Common Electrical: Common Electrical I/O (CEI) - Electrical and Jitter Interoperability agreements for 6G+ bps, 11G+ bps and 25G+ bps I/O," https://www.oiforum.com/wp-content/uploads/2019/01/OIF-CEI-04.0.pdf (2017).
14. R. Hui and M. O'Sullivan, Fiber Optic Measurement Techniques (Elsevier Science, 2009), chap. 2: Basic Instrumentation for Optical Measurement, pp. 129–258, 1st ed.
15. Keysight, "Application note: Equivalent Time Sampling Oscilloscope vs. Real-Time Oscilloscope," https://www.keysight.com/zz/en/assets/7018-01852/application-notes/5989-8794.pdf.
16. R. F. H. Fischer, Precoding and Signal Shaping for Digital Transmission (Wiley, 2002), chap. 2: Digital Communications via Linear Distorting Channels, pp. 14–85.
17. J. G. Proakis and M. Salehi, Digital Communications (McGraw-Hill Higher Education, 2008), chap. 10: Adaptive Equalization, pp. 689–705, 5th ed.
18. G. Simon, F. N. Sampaio, F. Saliou, J. Potet, and P. Chanclou, "Experimental Analysis of TDEC for Higher Speed PON Including Linear Equalization," in 2022 European Conference on Optical Communication (ECOC), (2022), pp. 1–4.
19. G. P. Agrawal, Nonlinear Fiber Optics (Elsevier, 2019), chap. 3: Group-Velocity Dispersion, pp. 57–84, 6th ed.
20. G. Caruso, I. N. Cano, G. Talli, D. Nesset, and R. Gaudino, "Study of TDEC for 50G-PON Upstream at 50 Gb/s in Negative Dispersion Regime using 25G-class Transceivers," in 2023 Optical Fiber Communications Conference and Exhibition (OFC), (2023), pp. 1–3.